Indonesian Journal of Science & Technology

Journal homepage: http://ejournal.upi.edu/index.php/ijost/

Optimization of Piper Trilinier Diagram Using Lithium Isotope Systematics: An Application for Detecting the Contribution of Geothermal Water from Aso Caldera after Earthquake 2016 in Kumamoto Aquifer, Japan

Rofiqul Umam[1,2,], Rahmad Junaidi[3], Muhamad Syazali[4], Fajri Farid[5], Antomi Saregar[6], A. Andiyan[7], Hirotaka Takahashi[8,9,10]*

[1]Faculty of Life and Environmental Sciences, University of Tsukuba, Japan
[2]Center for Research in Radiation, Isotopes, and Earth System Sciences (CRiES), University of Tsukuba, Japan
[3]Faculty of Science and Technology, Universitas Islam Negeri Sunan Ampel Surabaya, Indonesia
[4]Department of Mathematics, the Republic of Indonesia Defense University, Indonesia
[5]Data Science Study Program, Institut Teknologi Sumatera, Indonesia
[6]Department of Physics Education, Universitas Islam Negeri Raden Intan Lampung, Indonesia
[7]Faculty of Science and Engineering, Universitas Faletehan, Indonesia
[8]Department of Design and Data Science and Research Center for Space Science, Tokyo City University, Japan
[9]Institute for Cosmic Ray Research (ICRR), The University of Tokyo, Japan
[10]Earthquake Research Institute, The University of Tokyo, Japan
*Correspondence: E-mail: rofiqul.umam@ied.tsukuba.ac.jp

ABSTRACT

Optimization of the use of the Piper trilinear diagram was carried out by adding Lithium isotope systematics as a more accurate water-type analysis. The method used in this research is to analyze the Cl/Li ratio > 1000, δ^7Li < 10 ‰, and Lithium concentration of groundwater, and then the results of the analysis are integrated into a Piper trilinear diagram. The research results show that Lithium isotope systematics (Cl/Li ratio < 1000, δ^7Li < 10 ‰ and Li concentration) graph can be divided into 3 regions, namely geothermal water type has Cl/Li < 1000 and δ^7Li < 10 ‰, then shallow groundwater which has Cl/Li > 1000 but δ^7Li < 10 ‰ experienced natural contamination from geothermal waters, and fluid that has a Cl/Li ratio > 1000 and 10 ‰ > δ^7Li > 20 ‰ is estimated to be shallow groundwater.

ARTICLE INFO

Article History:
Submitted/Received 29 Nov 2024
First Revised 30 Dec 2024
Accepted 26 Feb 2025
First Available Online 27 Feb 2025
Publication Date 01 Apr 2025

Keyword:
Optimization,
Geothermal waters,
Lithium isotope systematics,
Piper trilinear diagram,
Shallow groundwater,
Water type analysis.

1. INTRODUCTION

Piper plots, commonly known as the Piper trilinear diagram**,** is a method that has been widely used in the field of geochemistry [1-2]. The use of this method is based on the content of ions such as Na^+, K^+, Mg^{2+}, Ca^{2+}, Cl^-, HCO_3^-, CO_3^{2-}, and SO_4^{2-} in groundwater, soil, and gas [3].

The Piper Trilinier diagram model is a very effective tool for the study of the separation of sources of dissolved elements in groundwater, changes or modifications to the properties of water passing through a certain area [4], and its relationship to geochemical problems [5]. The model analysis procedure is based on a ternary diagram that has been developed gradually through experimentation and shape modification [6]. This diagram consists of two equilateral triangles that are located below the right and left, where each is for plotting a cation on the one hand and an anion on the other.

At the top of the Piper trilinear diagram, there is a parallelogram plot that is connected between the two ternary diagrams, namely cations and anions. Based on the position of the points on the parallelogram, the type of groundwater chemistry can be interpreted [7].

Based on its division, the parallelogram plot in the Piper Trilinier diagram is divided into four dominant areas of fluid type. First, sodium chloride (NaCl) fluid is a type of fluid that comes from the sea, inside the earth (geofluids) and is released from the subduction process of the earth's plates [8]. Usually, high levels of sodium chloride are found in volcanic areas to be used as a tracer for geothermal energy potential. The Cl^- element is the main anion, but there are also other elements such as K^+, Na^+, Ca++, and Mg^{++}. Sodium chlorine also contains a high concentration of SiO_2 and has a neutral pH, which can be slightly acidic or alkaline [9]. The characteristic of sodium chlorine is the presence of amorphous silica because the water is saturated with silica [10].

Second, the type of sodium bicarbonate ($NaHCO_3$) fluid is the result of washing NaCl with fresh water $Ca(HCO_3)_2$. This occurs when seawater is trapped during the formation of the beach, and then the location is continuously irrigated by fresh water, resulting in the following chemical cation exchange reaction [10]. Based on a hydrostratigraphic perspective, this incident is very possible because the aquifer is in the same cyclical lithology, so fresh water that comes from rainwater or that is in the aquifer continuously flows into seawater and is trapped, resulting in a chemical reaction: $Ca(HCO_3)_2 + NaCl \longrightarrow CaCl_2 + NaHCO_3$. In addition, high HCO_3 and low Cl content can occur due to the presence of limestone rocks below the surface, which are characterized by travert ($CaCO_3$) deposits trapped around hot springs [11 – 14].

The third, calcium bicarbonate $Ca(HCO_3)_2$ fluid, is a type of freshwater that has not been contaminated with seawater, meaning that this type is an indication of groundwater that comes from rainwater and then enters the ground but does not undergo a heating process [15 – 16].

Fourth, calcium-magnesium bicarbonate ($CaMgCl_2$) fluid, is a type of fresh water that has been contaminated with carbonate. $CaMgCl_2$ has the meaning that this type is an indication of groundwater that comes from rainwater, and then enters the limestone or karst area but does not undergo a heating process [17].

Piper trilinear diagrams are often used to find types of fluids that have a mixture of complex compounds, such as major elements [18 – 19]. However, the use of the Piper trilinear diagram still has shortcomings in identifying more specific fluid types, for example, fluids with high sodium chlorine dominance. In terms of type classification, high levels of sodium chlorine can be found in seawater, geothermal water, slab-dehydrated fluids, and mixing waters [20].

DOI: https://doi.org/10.17509/ijost.v10i1.80974
p- ISSN 2528-1410 e- ISSN 2527-8045

However, many researchers still find it difficult to differentiate between slab-dehydrated fluids and seawater if the water samples are in coastal areas or even islands such as Hawaii [21 – 25].

In this research, optimization of the use of the Piper trilinear diagram was carried out by adding Lithium isotope systematics as a more accurate water type analysis. Analysis of several samples from different locations, shallow groundwater and Aso Caldera, Kumamoto, Japan (geothermal water), has been carried out to determine the effectiveness of using lithium isotope systematics.

2. METHODS

10 groundwater samples were taken from a confined aquifer, and one artesian well was collected along the eastern active groundwater direction in Kumamoto, Japan [26]. Groundwater samples collected on site are then placed in plastic (polypropylene) bottles that have been previously cleaned with ultrapure water [27]. Major elements were ascertained by titration and ion chromatography; fundamental information Li concentrations were measured by ICP-MS (ELAN DRCII, Perkin Elmer SCIEX, MA, USA); and Lithium isotopes were examined by ion chromatography and subsequently ICP-MS (ELAN DRCII, Perkin Elmer SCIEX, MA, USA). For four geothermal water samples, data were taken from previous research by [28], in the Sezaki area, Japan (**Table 1** and **Table 2**).

Table 1. Data on Lithium isotope systematics in this article has been taken from the previous article with various sources and types of water; geothermal water in Aso Caldera volcanoes, Japan [28], and shallow groundwater and river water in Kumamoto, Japan [26].

Fluid Type (Source)	Date and Location	Li (ppm)	Cl/Li	δ^7Li (‰)
Geothermal Water [28]	Aso Caldera Volcanoes, Japan	18.20	0.22	2.60
		23.60	0.07	9.00
		0.70	1.63	4.80
		1.50	0.12	7.64
Shallow Groundwater [26]	Shallow Groundwater (Confined aquifer) Kumamoto, Japan	0.0055	1472.72	20.00
		0.0061	1557.37	16.00
		0.0028	2892.85	7.20
		0.0029	3241.37	7.50
		0.0045	2977.77	15.70
		0.0045	3155.55	13.90
		0.0037	2243.24	7.30
		0.0037	2621.62	7.90
		0.0045	1800.00	8.60
		0.0044	2068.18	8.50

Table 2. Data on major elements in this article has been taken from the previous article with various sources and types of water; geothermal water in Aso caldera volcanoes, Japan [28], and shallow groundwater and river water in Kumamoto, Japan [26].

Fluid Type (Source)	Temp (°C)	Major Elements (mg/L)						
		Mg^{2+}	Na^{+}	K^{+}	Ca^{2+}	Cl^{-}	SO_4	HCO_3^{-}
Geothermal Water [28]	23.10	4.08	6.53	0.42	3.89	3.95	11.50	nm
	40.40	na	na	na	1.57	1.69	3.44	Nm
	19.60	0.29	0.46	0.08	0.95	1.14	1.42	Nm
	40.00	0.41	0.75	0.23	0.74	0.17	4.99	Nm
Shallow Groundwater [26]	nm	7.50	15.30	5.10	16.50	8.10	16.40	83.40
	nm	7.70	15.50	5.50	11.50	9.50	15.80	78.90

DOI: https://doi.org/10.17509/ijost.v10i1.80974
p- ISSN 2528-1410 e- ISSN 2527-8045

Table 2 (continue). Data on major elements in this article has been taken from the previous article with various sources and types of water; geothermal water in Aso caldera volcanoes, Japan [28], and shallow groundwater and river water in Kumamoto, Japan [26].

Fluid Type (Source)	Temp	Major Elements (mg/L)						
	(°C)	Mg^{2+}	Na^{+}	K^{+}	Ca^{2+}	Cl^{-}	SO_4	HCO_3^{-}
	nm	9.30	12.40	3.90	25.00	8.10	27.60	76.00
	nm	8.80	12.20	4.70	19.80	9.40	24.40	72.90
	nm	16.00	27.00	9.00	38.60	13.40	57.70	149.60
	nm	15.50	26.60	9.30	27.80	14.20	52.20	144.80
	nm	8.90	12.20	4.70	24.20	8.30	21.10	78.50
	nm	9.20	12.60	4.90	19.90	9.70	21.70	75.20
	nm	9.20	12.30	4.10	23.00	8.10	25.70	74.80
	nm	9.20	12.60	4.80	18.30	9.10	25.20	72.00

3. RESULTS AND DISCUSSION

The interpretation of several fluid sources as shown in **Figure 1** significantly showed the variations in each type of fluid. Piper diagrams also distinguished fluids based on the composition of the dominant chemical elements. The research by [28] showed that the interpretation using major elements also describes the water-rock interactions experienced by the fluid [10] and the rock structure around the site where the fluid appears [29]. Therefore, the difference in dominant composition is influenced by the rock structure in each research area.

Data on shallow groundwater were taken before and after the earthquake in 2016 from the aquifer of the largest groundwater area in Japan, namely Kumamoto **(Figure 2)** [26]. The results showed that shallow groundwater has a dominant composition, which is magnesium carbonate (Mg–HCO_3^{-}), where bicarbonate anion (HCO_3^{-}) is the main dominant composition **(Figure 1)**.

The geothermal water data were taken from volcanic areas, namely Aso caldera volcanoes Kumamoto, Japan (geothermal water) **(Figure 2)** [28]. Geothermal water has been described in previous research and was assumed to be derived from thermal waters or magmatic fluids. The Piper diagram interpretation of geothermal in this research has the same dominant plot composition, namely magnesium carbonate (Mg–HCO_3^{-}) **(Figure 1)**. The results showed that shallow groundwater and geothermal water have the same dominant composition, which is magnesium carbonate (Mg–HCO_3^{-}), where bicarbonate anion (HCO_3^{-}) is the main dominant composition **(Figure 1)**. This discovery indicated that the water-rock interaction experienced by each fluid source is due to the same rock structure [30 – 35]. Even though shallow groundwater and geothermal water in this case have the same dominant composition, deeper analysis is needed to determine the type of the two samples, "Do they have the same origin?".

The results of the interpretation using Li concentrations are shown in **Figure 3**. The **Figure 3** shows that geothermal waters have a higher Li concentration than shallow groundwater. The high concentrations of Li have been positively correlated with the research by [36], they analyzed the Cl and Li concentrations of several types of geofluids and obtained information that a Cl/Li ratio < 1000, specifically stems from geothermal waters have the characteristics of the fluids.

DOI: https://doi.org/10.17509/ijost.v10i1.80974
p- ISSN 2528-1410 e- ISSN 2527-8045

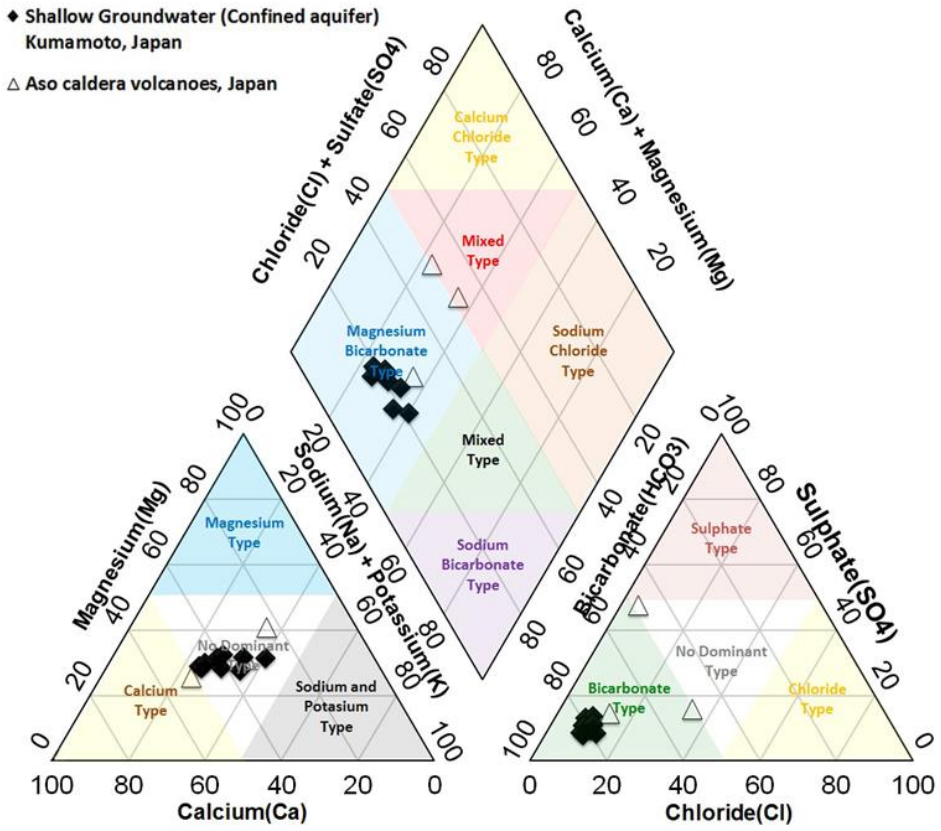

Figure 1. Interpretation of major elements of the sample fluids in the Piper trilinear diagram. Major elements describe fluid types based on their dominant composition. The transparent triangle is geothermal water data, while the black parallelogram is shallow groundwater data.

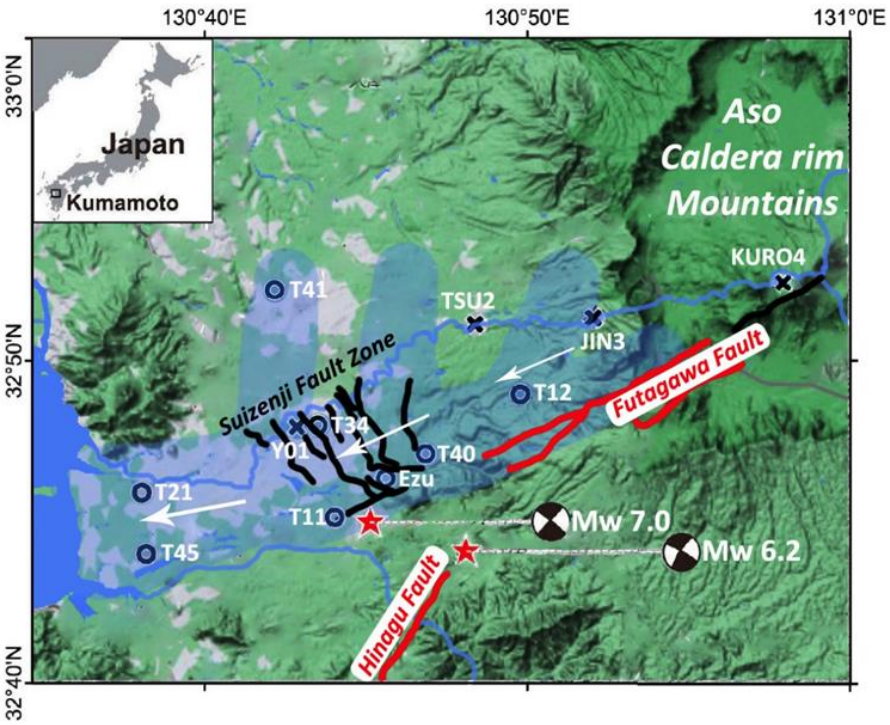

Figure 2. Location for sampling shallow groundwaters, river waters, and geothermal waters in Kumamoto, Japan.

DOI: https://doi.org/10.17509/ijost.v10i1.80974
p- ISSN 2528-1410 e- ISSN 2527-8045

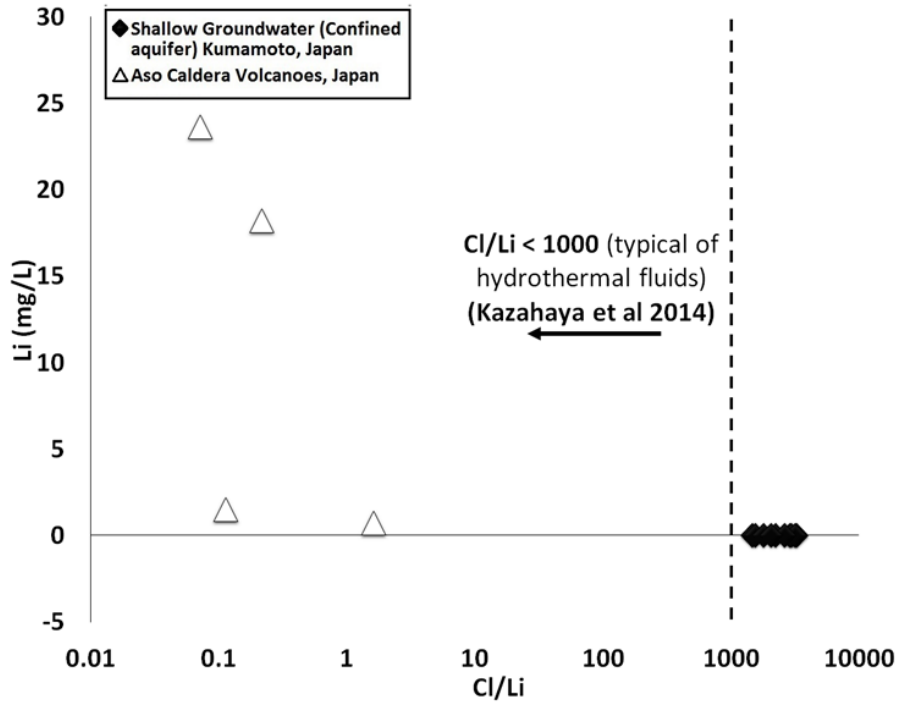

Figure 3. Li and Cl/Li ratio results. A high concentration of Li and Cl/Li ratio < 1000 is an indicator of typical hydrothermal/magmatic fluids [36].

Meanwhile, another interpretation using δ^7Li, and the Cl/Li ratio in **Figure 4**, showed that all geothermal waters have a Cl/Li ratio < 1000 with a value of δ^7Li < 10 ‰. Almost all geothermal waters also have a value of δ^7Li < 0 ‰, but two samples have a value of δ^7Li > 0 ‰. These results supported the natural isotope variation **(Figure 5)** [37 – 39], which showed that all geothermal waters have a value of δ^7Li is lower than shallow groundwater [37 – 41].

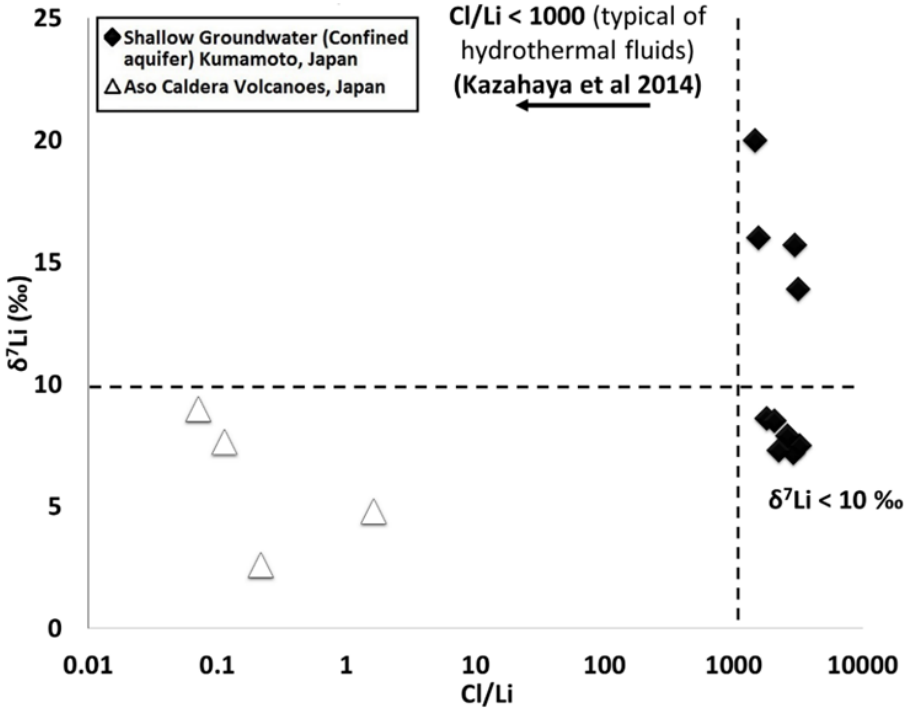

Figure 4. δ^7Li and Cl/Li ratio results. All of the geothermal waters have a value of δ^7Li < 10 ‰.

DOI: https://doi.org/10.17509/ijost.v10i1.80974
p- ISSN 2528-1410 e- ISSN 2527-8045

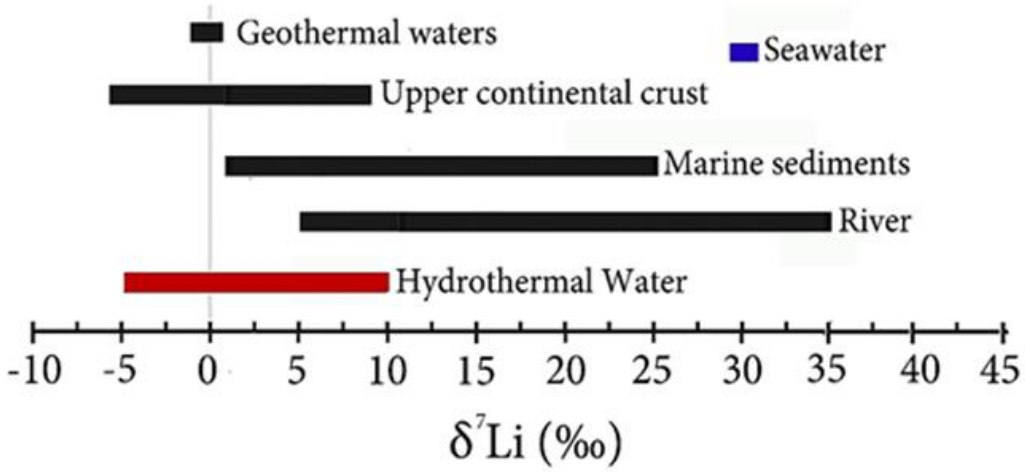

Figure 5. Isotopic variation of δ^7Li, modified from [39].

The percentage of mixed geothermal waters and shallow groundwater can be estimated using equations (1) and (2) below. This amplifies the contribution of geothermal waters that enter the shallow groundwater aquifers. The calculation uses concentrations and isotope ratios of the selected dissolved species (E) based on the two mixing components A and B in Equations (1) and (2):

$$E_M = E_A.f + E_B(1-f) \quad (1)$$

$$\delta E_M = \delta E_A.(E_A/E_M).f + \delta E_B.(E_B/E_M).(1-f) \quad (2)$$

where E_M, E_A, E_B, δE_M, δE_A, and δE_B are the concentrations and δ- values of mixed groundwater (M; T11 groundwater in 2016), geothermal waters (A), and shallow groundwater (B), respectively. The variable parameter f (from 0 to 1) was calculated from the best fit between *1/E* and δE.

The calculation using equations (1) and (2) produced a line/trend of the relative mixing between geothermal waters and shallow groundwaters **(Figure 6)**. The result of the line plot of mixing between geothermal waters and shallow groundwater [42] showed that there was almost no gradient change in the geothermal contribution percentage of 100% - 1% (region A). Furthermore, the shallow groundwaters in Region B have a geothermal water contribution of approximately 0.1%. The samples of shallow groundwaters in region C with isotope 10 ‰ < Li < 20 ‰ are estimated to be shallow groundwater.

By dividing 3 regions (A, B, and C) based on the Cl/Li < 1000 and δ^7Li < 10 ‰ lines **(Figure 6),** the correlation of major elements, namely Na^+, K^+, Mg^{2+}, Ca^{2+}, Cl^-, HCO_3^- and SO_4^{2-} **(Figure 7)**, it is estimated that shallow groundwater which has Cl/Li > 1000 but δ^7Li < 10 ‰ (region B) experienced natural contamination from geothermal waters. Meanwhile, the fluid that has a Cl/Li ratio > 1000 and an isotope value between 10‰ > Li > 20 ‰ (region C) is estimated to be shallow groundwater. This result strengthens the suspicion of previous research on several shallow groundwater aquifers in Kumamoto, Japan **(Figure 5)** that had natural contamination (deep groundwater) due to the 2016 major earthquake [26 – 28].

DOI: https://doi.org/10.17509/ijost.v10i1.80974
p- ISSN 2528-1410 e- ISSN 2527-8045

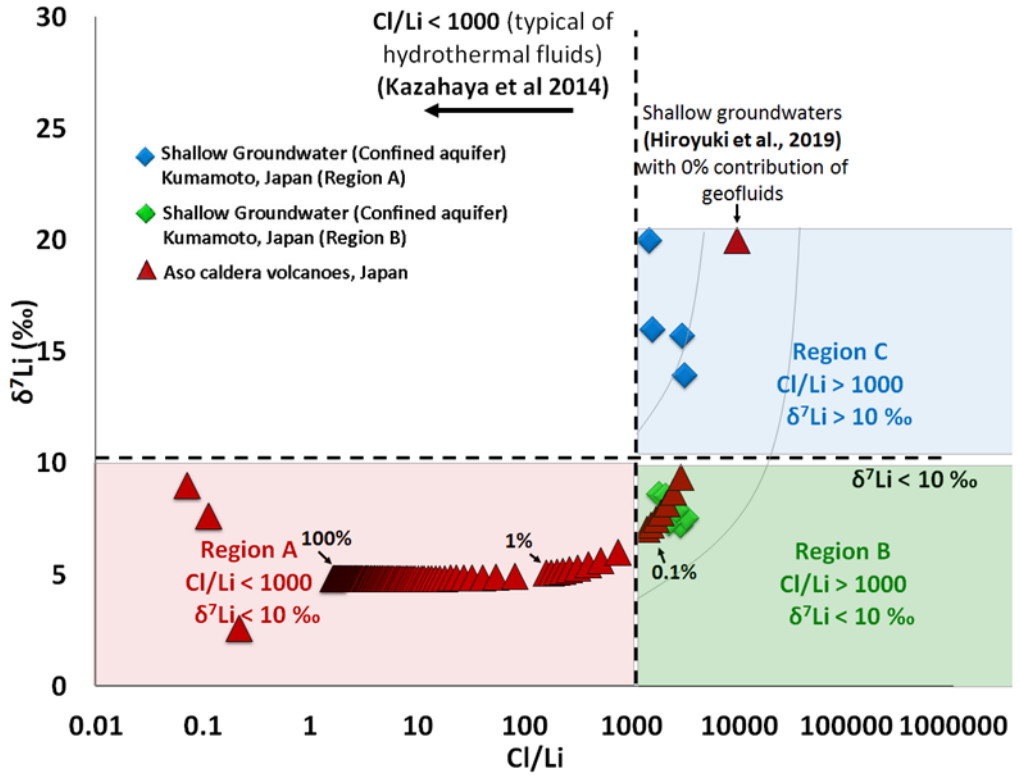

Figure 6. Contrasting feature of δ^7Li – Cl/Li between shallow groundwater and geothermal waters Aso Caldera Kumamoto, Japan.

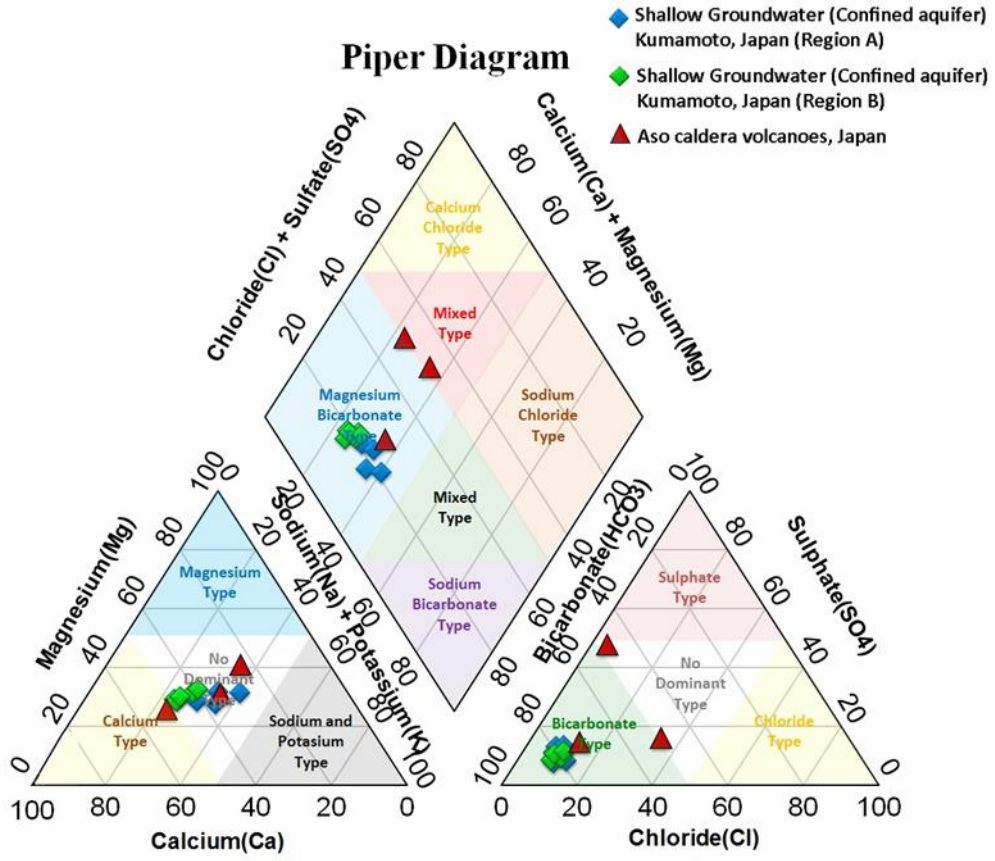

Figure 7. Piper trilinear diagram plot with red, green, and blue color indicators for region A, B, and C information.

DOI: https://doi.org/10.17509/ijost.v10i1.80974
p- ISSN 2528-1410 e- ISSN 2527-8045

4. CONCLUSION

The optimization of the Piper Trilinier diagram using Lithium isotope systematics provided clearer information on the type of fluid. The species differences between surface water, shallow groundwater, mixing water (contribution of 0.01% geothermal water), and geothermal waters can be fully understood after adding an interpretation of the concentration of Li and their isotopes. Based on the Cl/Li < 1000 and δ^7Li < 10 ‰ graph, we can divide 3 regions, namely A, B, and C, and then put them into the Trilinear Piper diagram to optimize water type analysis. The correlation of major elements, namely Na^+, K^+, Mg^{2+}, Ca^{2+}, Cl^-, HCO^{3-} and SO_4^{2-} and Lithium isotope systematics, no gradient change in the geothermal contribution percentage of 100% - 1% (region A), it is estimated that shallow groundwater which has Cl/Li > 1000 but δ^7Li < 10 ‰ (region B) experienced natural contamination from geothermal waters. Meanwhile, the fluid that has a Cl/Li ratio > 1000 and an isotope value between 10‰ > Li > 20 ‰ (region C) is estimated to be shallow groundwater. Even though shallow groundwater and geothermal water are located in the same piper plot (magnesium bicarbonate), Lithium isotope systematics can detect more clearly the differences in the types of these two samples. This result strengthens the suspicion of previous research on several shallow groundwater aquifers in Kumamoto, Japan, that had natural contamination (deep groundwater) due to the 2016 major earthquake. Furthermore, the differences in the fluid type between geothermal waters and shallow groundwater are visible using the Li isotopes.

5. ACKNOWLEDGMENT

The author would like to thank anonymous reviewers for their constructive reviews. The author would like to thank Ikuo Nishimura, Founder of Mandom Company Japan, for providing the Nishimura Foundation International Scholarship.

6. AUTHORS' NOTE

The authors declare that there is no conflict of interest regarding the publication of this article. The authors confirmed that the paper was free of plagiarism.

7. REFERENCES

[1] Sadashivaiah, C., Ramakrishnaiah, C. R., and Ranganna, G. (2008). Hydrochemical analysis and evaluation of groundwater quality in Tumkur Taluk, Karnataka State, India. *International Journal of Environmental Research and Public Health*, *5*(3), 158–164.

[2] Sadjab, B, A., Indrayana, I, P, T., Iwamony, S. and Umam, R. (2020). Investigation of the distribution and Fe content of iron sand at Wari Ino beach Tobelo using resistivity method with werner-schlumberger configuration. *Jurnal Ilmiah Pendidikan Fisika Al-Biruni, 9*(1), 141–160.

[3] Adejumo, R. O., Adagunodo, T. A., Bility, H., Lukman, A. F., and Isibor, P. O. (2018). Physicochemical constituents of groundwater and its quality in crystalline bedrock, Nigeria. *International Journal of Civil Engineering and Technology*, *9*(8), 887–903.

[4] Saparun, M., Akbar, R., Marbun, M., Dixit, A. and Saxena, A. (2022). Application of induced polarization and resistivity to the determination of the location of minerals in extrusive rock area, Southern Mountains of Java, Indonesia. *International Journal of*

Hydrological and Environmental for Sustainability, *1*(3), 108–119.

[5] Saxena, A., Panse, V, R., Asyhari, A., Umam, R., Domańska, M, M. and Dixit, A. (2024). Modifying the DC servo motor observed by particle swarm optimization techniques. *International Journal of Electronics and Communications System, 4*(2), 113–125.

[6] Sabara, Z., Anwar, A., Yani, S., Prianto, K., Junaidi, R., Umam, R. and Prastowo, R. (2022). Activated carbon and coconut coir with the incorporation of abr system as greywater filter: The implications for wastewater treatment. *Sustainability, 14*(2), 1026.

[7] Umar Kura, N., Firuz Ramli, M., Azmin Sulaiman, W. N., Ibrahim, S., Zaharin Aris, A., and Mustapha, A. (2013). Evaluation of factors influencing the groundwater chemistry in a small tropical Island of Malaysia. *International Journal of Environmental Research and Public Health*, *10*(5), 1861–1881.

[8] Rajindra, R., Wekke, I, S., Sabara, Z., Pushpalal, D., Samad, M, A., Yani, A. and Umam, R. (2019). Diversity, resilience, and tragedy: Three disasters in Palu of Indonesia, *International Journal of Innovation, Creativity and Change, 5*(2), 1592 – 1607.

[9] Tsay, A., Zajacz, Z., Ulmer, P., and Sanchez-Valle, C. (2017). Mobility of major and trace elements in the eclogite-fluid system and element fluxes upon slab dehydration. *Geochimica et Cosmochimica Acta*, *198*, 70–91.

[10] Chae, G. T., Yun, S. T., Kim, K., and Mayer, B. (2006). Hydrogeochemistry of sodium-bicarbonate type bedrock groundwater in the Pocheon spa area, South Korea: water-rock interaction and hydrologic mixing. *Journal of Hydrology*, *321*(1–4), 326–343.

[11] Kimura, K. (1990). Formation mechanism of high sodium bicarbonate groundwater in landslide areas in the Kobe Group. *Journal of Groundwater Hydrology*, *32*(1), 5–16.

[12] Al-Qawati, M., El-Qaysy, M., Darwesh, N., Sibbari, M., Hamdaoui, F., Kherrati, I., El Kharrim, K., and Belghyti, D. (2018). Hydrogeochemical study of groundwater quality in the west of Sidi Allal Tazi, Gharb area, Morocco. *Journal of Materials and Environmental Science*, *9*(1), 293–304.

[13] Bhat, M. A., Wani, S. A., Singh, V. K., Sahoo, J., Tomar, D., and Sanswal, R. (2018). An Overview of the Assessment of Groundwater Quality for Irrigation. *Journal of Agricultural Science and Food Research*, *9*(1), 1–9.

[14] Furuya, K., and Harada, K. (1995). An automated precise Winkler titration for determining dissolved oxygen on board ship. *Journal of Oceanography*, *51*(3), 375–383.

[15] Rufaidah, E., As'atirsyadi, K., Saregar, A. and Umam, R. (2018). The effect of halal label to increase domestic and international tourism: Case study in Lombok, Indonesia, *International Journal of Management and Business Research, 8*(4), 29-36.

[16] Acharya, S., Sharma, S. K., and Khandegar, V. (2018). Assessment of groundwater quality by water quality indices for irrigation and drinking in South West Delhi, India. *Data in Brief*, *18*(2018), 2019–2028.

[17] Al-Ghamdi, A. Y., Saraya, M. E. S. I., Al-Ghamdi, A. O., and Zabin, S. A. (2014). Study of physico-chemical properties of the surface and ground water. *American Journal of Environmental Sciences*, *10*(3), 219–235.

[18] Akoteyon, I. S. (2013). Hydrochemical studies of ground water in parts of lagos,

DOI: https://doi.org/10.17509/ijost.v10i1.80974
p- ISSN 2528-1410 e- ISSN 2527-8045

southwestern Nigeria. *Bulletin of Geography. Physical Geography Series*, *6*(1), 27–42.

[19] Idroes, R., Yusuf, M., Saiful, S., Alatas, M., Subhan, S., Lala, A., Muslem, M., Suhendra, R., Idroes, G. M., Marwan, M., and Mahlia, T. M. I. (2019). Geochemistry exploration and geothermometry application in the North Zone of Seulawah Agam, Aceh Besar District, Indonesia. *Energies*, *12*(23), 4442.

[20] Iqbal, M., Kusumasari, B. A., Atmapradhana, T., Trinugraha, A. C., Palupi, E. K., and Maulidi, I. (2023). Characterization of thermal waters origin from the back arc lampung province, Indonesia : an evaluation of stable isotopes, major elements, and li / cl ratios. *International Journal of Hydrological and Environmental for Sustainability*, *2*(1), 1–12.

[21] Sabara, Z., Afiah, I, N. and Umam, R. (2022). Integration of Green Ergonomics in Robust Decision Making Approach in Water Resources Management in Makassar City, *International Journal of Technology, 13*(2), 264 - 273.

[22] Stern, R. J. (2018). The evolution of plate tectonics. *Philosophical Transactions of the Royal Society A: Mathematical, Physical and Engineering Sciences*, *376*(2132).

[23] Zoysa, R. S. De, Schöne, T., Herbeck, J., Illigner, J., Haghighi, M., Simarmata, H., Porio, E., Rovere, A., and Hornidge, A. K. (2021). The "wickedness" of governing land subsidence: Policy perspectives from urban southeast Asia. *PLoS ONE*, *16*(6), 1–25.

[24] Chorus, I., and Bartram, J. (1999). Toxic Cyanobacteria in Water: A guide to their public health consequences, monitoring and management. *In Cytometry Part A, 95*(8).

[25] Jasechko, S., Perrone, D., Seybold, H., Fan, Y., and Kirchner, J. W. (2020). Groundwater level observations in 250,000 coastal US wells reveal scope of potential seawater intrusion. *Nature Communications*, *11*(1), 1–9.

[26] Tanimizu, M., Sugimoto, N., Hosono, T., Kuribayashi, C., Morimoto, T., Ito, A., and Umam, R. (2021). Application of B and Li isotope systematics for detecting chemical disturbance in groundwater associated with large shallow inland earthquakes in Kumamoto, Japan. *Geochemical Journal, 55(4), 241-250.*.

[27] Umam, R., Tanimizu, M., Nakamura, H., Nishio, Y., Nakai, R., Sugimoto, N., Mori, Y., Kobayashi, Y., Ito, A., Wakaki, S., Nagaishi, K., and Ishikawa, T. (2022). Lithium isotope systematics of Arima hot spring waters and groundwaters in Kii Peninsula. *Geochemical Journal*, *56*(5), 8–17.

[28] Hosono, Takahiro, Hartmann, J., Louvat, P., Amann, T., Washington, K. E., West, A. J., Okamura, K., Böttcher, M. E., and Gaillardet, J. (2018). Earthquake-induced structural deformations enhance long-term solute fluxes from active volcanic systems. *Scientific Reports*, *8*(1), 1–12.

[29] Shiomi, K., and Park, J. (2008). Structural features of the subducting slab beneath the Kii Peninsula, central Japan: Seismic evidence of slab segmentation, dehydration, and anisotropy. *Journal of Geophysical Research: Solid Earth*, *113*(10), 1–13.

[30] Giggenbach, W. F. (1991). Chemical techniques in geothermal exploration. In *Chemistry Division, 1991*, 119–144.

[31] Hosono, T., Yamada, C., Shibata, T., Tawara, Y., Wang, C. Y., Manga, M., Rahman, A. T. M. S., and Shimada, J. (2019). Coseismic groundwater drawdown along crustal ruptures

DOI: https://doi.org/10.17509/ijost.v10i1.80974
p- ISSN 2528-1410 e- ISSN 2527-8045

during the 2016 mw 7.0 kumamoto earthquake. *Water Resources Research*, *55*(7), 5891–5903.

[32] Hosono, Takahiro, and Masaki, Y. (2020). Post-seismic hydrochemical changes in regional groundwater flow systems in response to the 2016 Mw 7.0 Kumamoto earthquake. *Journal of Hydrology*, *580*(2020), 124340.

[33] Kawabata, K., Sato, T., Takahashi, H. A., Tsunomori, F., Hosono, T., Takahashi, M., and Kitamura, Y. (2020). Changes in groundwater radon concentrations caused by the 2016 Kumamoto earthquake. *Journal of Hydrology*, *584*(February), 124712.

[34] Hosono, Takahiro, Tokunaga, T., Tsushima, A., and Shimada, J. (2014). Combined use of δ13C, δ15N, and δ34S tracers to study anaerobic bacterial processes in groundwater flow systems. *Water Research*, *54*, 284–296.

[35] Hosono, Takahiro, Yamada, C., Manga, M., Wang, C. Y., and Tanimizu, M. (2020). Stable isotopes show that earthquakes enhance permeability and release water from mountains. *Nature Communications*, *11*(1), 1–9.

[36] Kazahaya, K., Takahashi, M., Yasuhara, M., Nishio, Y., Inamura, A., Morikawa, N., Sato, T., Takahashi, H. A., Kitaoka, K., Ohsawa, S., Oyama, Y., Ohwada, M., Tsukamoto, H., Horiguchi, K., Tosaki, Y., and Kirita, T. (2014). Spatial distribution and feature of slab-related deep-seated fluid in SW Japan, *日本水文科学会誌*, *44*(1), 3–16.

[37] Millot, R., Hegan, A., and Negrel, P. (2012). Geothermal waters from the Taupo Volcanic Zone, New Zealand: Li, B, and Sr isotopes characterization. *Applied Geochemistry*, *27*, 677–688.

[38] Prastowo, R., Ipmawan, V, L., Zamroni, A., Umam, R., Permanasari, I, N, P. and Siregar, R, N. Identification of ground motion prone areas triggering earthquakes based on microtremor data in Jati Agung district, South Lampung Regency, Lampung, Indonesia. *AIP Conference Proceedings, 2245*(2020), 70003.

[39] Tomascak, P. B. (2004). Developments in the understanding and application of lithium isotopes in the earth and planetary sciences. *Reviews in Mineralogy and Geochemistry*, *55*(1), 153–195.

[40] Millot, R., Negrel, P., and E Petelet, giraud. (2007). Multi-isotopic (Li, B, Sr, Nd) approach for geothermal reservoir characterization in the Limagne Basin (Massif Central, France). *Applied Geochemistry*, *22*(11), 2307–2325.

[41] Meredith, K., Moriguti, T., Tomascak, P., Hollins, S., and Nakamura, E. (2013). The lithium, boron and strontium isotopic systematics of groundwaters from an arid aquifer system: Implications for recharge and weathering processes. *Geochimica et Cosmochimica Acta*, *112*, 20–31.

[42] Umam, R.,Cengiz, K. and Said, A. (2024). Application of major and trace elements for detecting the origin of groundwater: Lithium enrichment in ain al-harrah hot spring influenced by Red Sea, Saudi Arabia. *International Journal of Hydrological and Environmental for Sustainability*, 3(3), 151-162.

DOI: https://doi.org/10.17509/ijost.v10i1.80974
p- ISSN 2528-1410 e- ISSN 2527-8045